Marine Structures 103 (2025) 103793

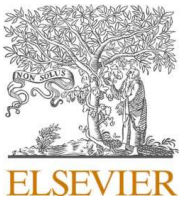

Contents lists available at ScienceDirect

Marine Structures

journal homepage: www.elsevier.com/locate/marstruc

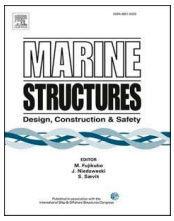

Experimental and numerical assessment of ultimate strength of a transversally loaded thin-walled deck structure

Beatrice Barsotti [a], Carlo Battini [b], Marco Gaiotti [a], Cesare Mario Rizzo [a,*], Gianmarco Vergassola [a]

[a] University of Genova, Polytechnic School, DITEN - via Montallegro 1, Genova 16145, Italy
[b] University of Genova, Polytechnic School, DICCA - via Montallegro 1, Genova 16145, Italy

ARTICLE INFO

Keywords:
Stiffened panel
Buckling
Ultimate strength
Collapse
Large-scale test
Nonlinear analysis

ABSTRACT

Many studies have been conducted to determine the ultimate strength of axially loaded ship structures at different levels of complexity, considering grillages, stiffened panels, transverse ring frames as well as complete hull blocks, aimed at assessing progressive collapse analysis of the whole hull girder, both analytically and numerically. However, little research has been conducted on the effects that transversal loads can have on relatively thin shell plating, particularly sensitive to buckling phenomena even for rather low loading thresholds. Moreover, the more and more frequent use of higher and higher strength steels makes ship structures slender and, consequently, likely to be even more sensitive to buckling phenomena. In the framework of a research project funded by Fincantieri R&D Department, a full-scale experimental test is performed on a structure simulating a deck portion characterized by a relatively thin plating, such as to induce an early local elastic buckling with a wide post-buckling range, before the ultimate load is reached. Nonlinear finite element analysis is carried out to design the experiment, considering both the nominal and the actual geometry of the structure as obtained by laser scanning the plating and by 3D reconstruction of the stiffeners. The effect of initial plating imperfection and of welding residual stresses on the numerical models has been considered as well, verifying their impact both, on the load end-shortening curve and on the ultimate strength of the panel.

1. Introduction

A reliable evaluation of the ultimate strength capacity of ships and offshore structures is crucial for assessing the structural response against extreme events and accidental loads. However, the use of finite element software for the solution of complex non-linear problems is still limited in actual design practices of shipyards and design offices for these applications. Instead, simpler analytical methods such as Smith's method are preferred, also because nonlinear Finite Element Analyses (FEA) results are very sensitive to the input parameters and to the solution algorithms applied. In fact, the ISSC 2022 committee III.1 on Ultimate Strength reports that there are sources of uncertainties related to physical characteristics, modelling assumptions and human factor introduced by the analyst that significantly affect the FEA results accuracy [1].

Moreover, the need to assess the degree of accuracy of numerical or analytical approaches to predict the ultimate response of marine structures led the ISSC 2022 committee III.1-Ultimate Strength to conduct a broad blind-benchmark on the subject [2], also

* Corresponding author.
E-mail address: cesare.rizzo@unige.it (C.M. Rizzo).

https://doi.org/10.1016/j.marstruc.2025.103793
Received 24 October 2024; Received in revised form 26 January 2025; Accepted 3 February 2025

presenting a discussion on the participants' ability to predict the results of a reference experiment with the (limited) offered information analogous to those available at the ship preliminary design stage.

In the reported benchmark, the ISSC 2022 III.1-Ultimate Strength emphasizes the importance of considering the entire end-shortening curve of the specimen, rather than solely concentrating on the specific point that determines its ultimate capacity [1]. The influence of this factor can have a significant impact on situations where energy plays a dominant role in the physics of the problem. This is often the case in scenarios involving collapse phenomena such as hull girder progressive failure due to wave loading effects [3] or progressive collapse of stiffened panels. In recent literature, the hull girder ultimate strength or that of its components is also discussed in the context of more complex problems, such as considering combined loads [4–6], cyclic loads [7,8], dynamic response [9,10], and damaged [11,12] or degraded ships [13]. However, such highly complex numerical analyses are often poorly supported by experimental validations, and, at best, they are limited to provide sensitivity of the applied model to the input parameters.

The effect of transverse loads on thin-walled ship's structures is even more often treated to a limited extent being only considered as one of the acting load components in the context of multi-axial loading studies causing the reduction of the ultimate axial capacity of the structure. In the literature, such analyses are generally again carried out at a numerical level only [14], given the complexity of realizing multi-axial experimental setups [15], thus lacking experimental validation of the proposed models.

On the other hand, a few ship construction rules imply elastic instability limit state of elementary plate panels [16,17], possibly not being able to exploit the scantling advantages of the use of high strength steels.

Although transversal stresses are generally rather low on ship structures, the longitudinal extension of the elementary shell plating panels, combined with their small thickness, leads to very low thresholds of critical stresses. As a result, the compression of the deck caused by the hydrostatic load on the sides could potentially result in local buckling problems under elastic conditions, especially when combined with other design loads. Furthermore, the shipbuilding industry is increasingly turning to high-strength steels to meet the demand for lighter hulls. Consequently, this shift leads to the use of progressively thinner plates to withstand applied loads. However, although the yield strength of these materials increases, the same cannot be said for their stiffness, particularly the Young's modulus. This implies that designing slender structures poses significant challenges, particularly in terms of elastic buckling.

Even though transverse loads are not typically very high for ships with longitudinal structures, the strength against elastic instability can still be relatively low because of the aspect ratio of the elementary plating panels. As evidence of this, the regulatory framework designed to govern the formulas for verifying buckling with transverse stress components remains a topic of significant debate within the relevant international forums [18]. Thanks to a research project funded by Fincantieri, a decision was made to design a test geometry capable of assessing the structural behaviour of a relatively slender naval vessels structure in real scale, when subjected to transverse loads, perpendicular to the direction of the ordinary stiffeners. This structure is intentionally designed to induce local elastic instability at very low load levels compared to its ultimate capacity. The objective is to provoke an early nonlinear response in the resulting end-shortening curve, which would offer valuable insights into how the load is redistributed among the various structural components of the structure.

In order to accept loading conditions that involve local buckling of specific structural elements, it is essential to secure reliable experimental validation of predictive models. This involves assessing the residual response after surpassing the critical load threshold of individual components, focusing on both, the margin related to the overall structure's ultimate capacity and the resulting stiffness loss. Hence, a rather complex test design stage was necessary, involving several numerical simulations based on information and assumptions that have been validated only after the test was carried out.

The objective in this work was not only to evaluate the ultimate strength of the panel but also to understand the load redistribution among structural members due to local elastic instability of the plating. As mentioned, the transverse compression of the sides of a hull induces a small transverse axial compression, which may exceed the elastic buckling limit of the elementary panel due to the thin plating of the deck and the unfavourable aspect ratio of the panel in this direction.

In summary, in an attempt to overcome the currently required structural assessment framework, based on the critical threshold imposed by elastic buckling to all structural components individually and leading towards a limit state assessment based on the actual capacity reserve of the whole structure, it is necessary to be able to predict the post-buckling response and the interaction among structural components of stiffened panels, namely elementary plate panels and stiffening members, reliably and precisely.

In this study, an experimental-numerical comparison offers insights for an application case that has not been sufficiently and comprehensively considered, but it is certainly of interest in real-world hull structures. The research proposed here includes both experimental and numerical analyses of compressive transverse loads on a stiffened panel. Specifically, the experimental campaign focuses solely on transverse loading, featuring a test design tailored for collapse under such loading scenario and boasting a prolonged post-critical capacity. The specimen has been designed on purpose to obtain a particular buckling behaviour, using several FEA models before the panel was actually built; only thereafter the test was carried out and experimental results were analysed following various assumptions to exploit the experimental information.

The tested specimen has been designed with the same specifications of a real deck structure of a naval vessel and built up by a shipyard adopting usual shipbuilding techniques. In short, the scantlings were adapted to obtain a representative stiffened panel specimen, suitable to obtain the required buckling behaviour. A second round of FEA has been developed after the test in order to find the better simulation scenario for further deepening the collapse behaviour of the stiffened panel.

Moreover, this study originated a blind benchmark in which multiple international research institutions analysed the same geometry with the aim of comparing nonlinear numerical modelling approaches adopted in progressive collapse analysis. Preliminary results of the benchmark are reported in [19].

Validation of the numerical model was achieved through a meticulous process involving incremental adjustments to the model,

materials, and initial conditions. This validation was conducted against extensive experimental analyses of the collapse behaviour of a stiffened panel on a large scale. Furthermore, the study underscores the significant influence of initial imperfections, which markedly reduce stiffness, contrasting starkly with findings from previous studies.

2. Test and specimen design

The panel's geometry has been specifically designed to achieve early local elastic buckling, followed by a significant post-buckling phase, prior to reaching the ultimate load. This design also considers the overall dimensions of the laboratory test bench.

The dimensions and thicknesses of all the structural elements of the panel are listed below:

- *Plates*: t_1= 8 mm, t_2= 4mm. Where t_1 represents the thickness of plating extending longitudinally 800 mm from the ends and t_2 the one of the central part of the panel;
- *L-bars*: 60 × 5 × 30 × 5 mm (h_w x t_w x b_f x t_f), transverse ordinary stiffeners (y axis in Fig. 1);
- *T-bars*: 150 × 6 × 100 × 6 mm, transverse main stiffeners which extend, as L-shaped, also longitudinally (x axis in Fig. 1) along the longer edge of the panel obtaining a ring shape.

It was decided to adopt different thicknesses of plating to prevent collapse at the ends of the panel and enhance the clarity of the experimental investigation area. The panel was designed to be consistent with a typical deck structure of a ship. It must be again noted that, for the aim of this research, the main focus was devoted to the pre and post buckling behaviour, especially in the redistribution of stresses in the structure, rather than on the ultimate strength capacity.

The panel specimen is shown in Figs. 1 and 2. In particular, in Fig. 2, difference in size between transverse ordinary stiffeners (L bars) and longitudinal reinforced beams (T bars) can be noted. This geometry reveals to be suitable for this study, among several others analysed, since it brings the structure to a very early local instability as shown in the plots of Fig. 3. Three load end shortening curves are compared, in order to preliminary analyse the effects of two types of imperfections, i.e. 1st buckling mode shape and thin-horse shape. In Table 1 the resulting numerical curves are compared.

This first round of numerical simulations was necessary in order to deepen the structural response of the panel and for verifying if the specimen was properly designed for the purpose of investigating the ultimate strength. Moreover, it was necessary to understand if the panel was matching the maximum carrying capacity of the laboratory equipment. Since the panel was not already fabricated, the first round of simulations was done using its nominal characteristics.

In the plot of Fig. 3, it is possible to compare the structural response of the perfect model to that of the imperfect one, trying to identify the influence of two distinct patterns of imperfections. In one case an imperfection based on the 1st Eigen-mode with a maximum amplitude of 2 mm is assumed (Fig. 4), while in the other case a sinusoidal thin-horse imperfection on the plates, achieved through an imposed lateral pressure, has been applied to obtain a maximum lateral displacement of 2 mm (Fig. 5a). In Fig. 5a, the thin-horse shape is superimposed to the global bending effect while the thin-horse shape deformation of a bay is evidenced in Fig. 5b. The 2 mm displacement has been selected according to DNV-GL class guidelines [20], that suggests modelling the plate imperfections in the following way:

$$\text{Plates} : w_p = \frac{s}{200}$$

where s is the spacing of ordinary stiffeners.

This analysis has been done in the initial stage of this research in order to understand which deformation pattern better simulates the real imperfection acquired via laser scanning.

Numerical findings were derived through finite element method (FEM) numerical assessments utilizing ADINA software [21]. Specifically, static non-linear collapse analyses were conducted on the numerical model by applying a progressive axial compressive load to one end of the panel, while the other end was constrained by the testing bench stiffening structure. This preliminary numerical evaluation was performed to facilitate the design of the experimental test. The meshing parameters, i.e. type of element, mesh density and the material model and boundary conditions are also defined following the DNV-GL guideline report [20], which deals with the nonlinear FEA of stiffened panels. It also provides information and instructions about element type, mesh density and load application as it follows:

- MITC4-nodes quadrilateral shell elements of 25 mm x 25 mm are used
- The HSLA steel material is modelled by the elasto-plastic bilinear model with isotropic hardening, considering the results of the work reported in [22,23] and using the following mechanical characterization:
  - Young's modulus, E [N/mm^2] = 205,000
  - Poisson ratio, ν= 0.3
  - Yield stress [N/mm^2] = 355
  - Strain hardening parameter, ET [N/mm^2] = 1025
- The panel is fixed on one edge (x,y,z translations are fixed) at four points, i.e. where the load cells are installed (Fig. 6b). In Fig. 6, the boundary conditions applied in the model are reported as a matrix of the free (checks), fixed (bars) or constrained via rigid link

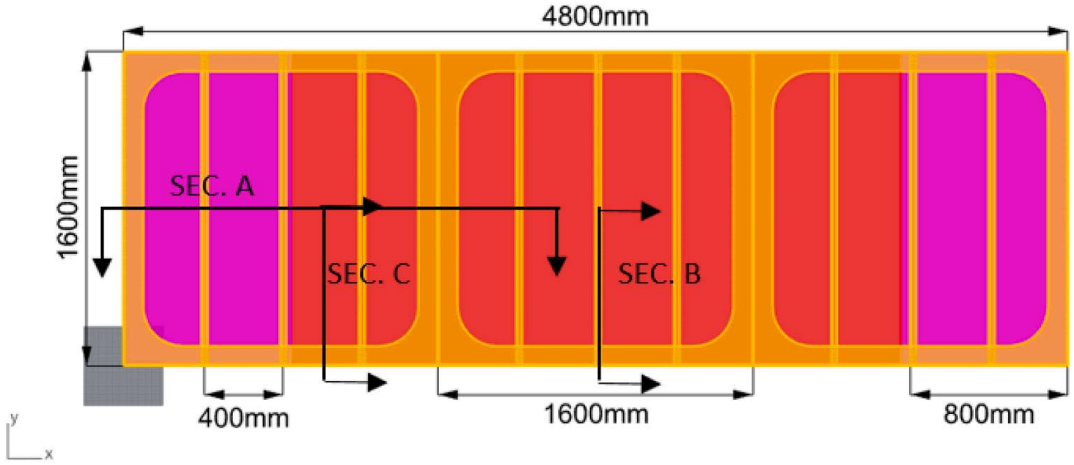

SECTION A

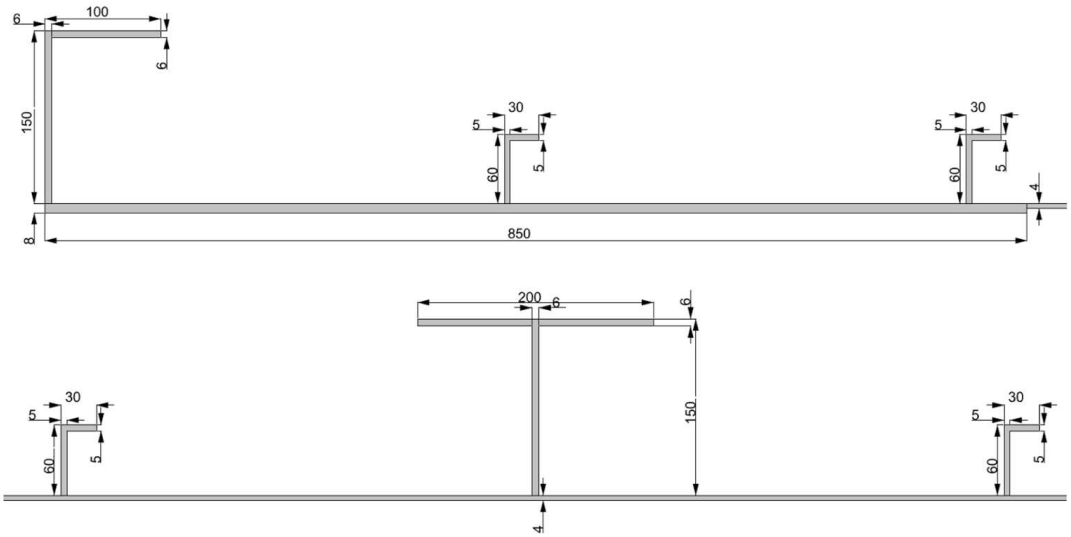

SECTION B

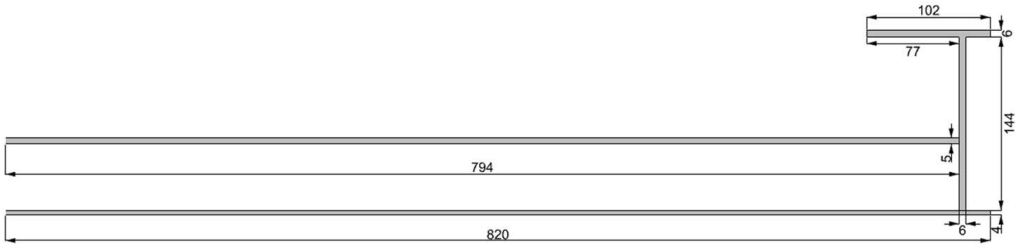

SECTION C

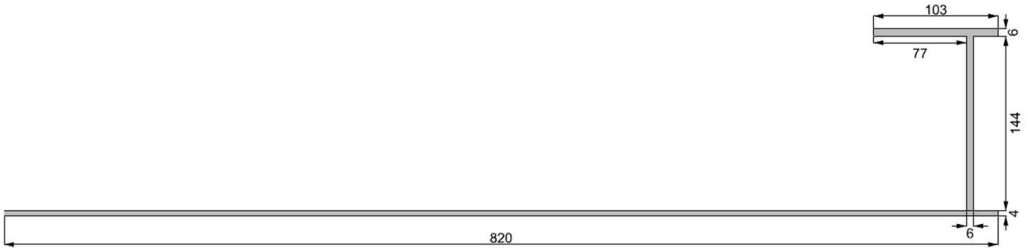

(caption on next page)

Fig. 1. Overall dimensions of the panel specimen and x, y-sections.

("C") degrees of freedom with respect to the zone where they have been applied (condition B, C or D). The same will apply for Fig. 24.

- The panel is free to translate in the longitudinal x-direction on the other edge, i.e. the one where the load is applied by the actuators (Fig. 6a). The experiment was devised to ensure an infinitely rigid plate at the loaded end, pushed axially by two actuators. The rigid constraint was meticulously designed and constructed to impart load without inducing end rotations, ensuring that displacements are rigidly transmitted to the panel. In the numerical model, this is faithfully replicated through the utilization of rigid links. These constraints ensures that the position of the load application point does not affect the results, as rigid links uniformly distribute forces and moments across all considered nodes. In particular, the axial compressive load is applied on the master node, which allows to transfer forces on all the slave nodes on the end plate of the panel specimen (Fig. 6a).

3. Actual imperfect geometry, thicknesses and material properties

Prior to conducting the experimental test, it is essential to conduct initial measurements on the structure. These measurements serve the purpose of making more reliable predictions and gaining a deeper understanding of the test results. Specifically, accurate determination of the actual geometry of the specimen is crucial due to the significant impact of initial geometric imperfections on the elastic buckling response of thin-walled structures. These imperfections can lead to notable discrepancies in the locations where the collapse process begins and the type of resulting failure. In addition to laser scanning to identify geometric imperfections, thickness measurements were carried out using an OMNI-TM-8812 ultrasonic probe.

Finally, once the test specimen was constructed, the material data for the steel plates used in its fabrication became available, including tensile tests carried out on multiple specimens, allowing for the material properties to be updated with the more accurate information.

Hence, the numerical model could be significantly improved both in terms of geometry and mechanical properties, highlighting the areas of interest where it is worth, e.g., to install strain gauges or to use DIC (Digital Image Correlation) technology.

3.1. Determination of geometric imperfections by laser scanning

The laser scanning technique was employed to reconstruct the surface of the panel, which represents the ideally flat portion of the specimen and constitutes its shell plating. The survey of the panel in its entirety was carried out using the $Z + F$ Imager5006 h phase shift scanner. This instrument acquires information up to 79 m with an acquisition range of 360° horizontally and 310° vertically. Operation involves sending a laser into the nodes of a spherical grid defined according to the density chosen by the user. The higher the density, the more points will be acquired by the instrumentation. Phase shift scanners emit laser light at alternating frequencies and measure the difference between the emitted and reflected signals to determine the distance to an object. Factors that can lead to an imperfect survey by the instrumentation can be the type of material being measured and the reflection angle of the laser.

In the specific case of the tested panel, some points were detected with a high error, which was easily filtered out in the post processing. Having then acquired four scanning locations, the next step was to align the scans into a single reference system. This process was carried out in two steps: the first saw the alignment of the scans, in the form of a point cloud, encompassing the entire area acquired, while the second was necessary to optimize any errors by isolating the panel and using surface alignment algorithms. Having thus defined the model, the next steps were to filter the data to eliminate scattered points affected by incorrect laser reflections. The points thus filtered were the basis for the generation of the mesh surface of the panel.

The stiffeners imperfections are obtained by using a portable 3D laser scanner (SHINING 3D), which allows a complete detection of geometric defects of parts of the specimen structure, providing as a result a CAD-type file showing all the acquired measurements [24]. This technique is suitable for reconstructing only relatively small objects, hence a full 3D reconstruction of all stiffeners was not possible. Three areas were selected for each stiffener, namely the two ends and the mid-span, and then reconstructed to evaluate the tilt angle at these three locations. In Fig. 7, an example of the output scan file is shown. The scanning of the stiffeners is in fact useful for understanding the angle of rotation of the stiffeners (i.e. tilt angle). It results that the rotation, i.e. this geometrical imperfection, is actually very small and such as not to influence the results of the numerical model.

After getting the CAD files containing the actual geometry, the FEM numerical model was updated to account for the initial imperfections. In particular, the panel lateral deviations from best-fit plane (the one that minimizes the deflection in all the measurement points, i.e. the average plane) are considered (see Fig. 8): given the difficulty to obtain the perfect coincidence between the imperfect CAD model points and the FEM nodes, it was decided to slightly smooth the actual geometry when updating the numerical model. The resulting geometry is then imported as initial imperfection for the FEM collapse analysis.

Fig. 8 also clearly shows that the detected shape of the initial deflection of the experimental sample is, unexpectedly, nowhere near the hungry horse mode. On the contrary, it looks rather similar to the mode-1 buckling shape, at least in the central part of the structure. This is likely due to elastic buckling that possibly occurred during the construction of the specimen. The test specimen, made of thin plates compared to the decks of ordinary merchant ships but in line with those of naval vessels, is considered to have buckled during fabrication process, resulting in different initial deflection characteristics, being the initial deflection of thin-horse mode more dominant for merchant ships [25].

It is important to underline that the critical elastic buckling load evaluated by FEA corresponds to an axial stress of 27.80 MPa,

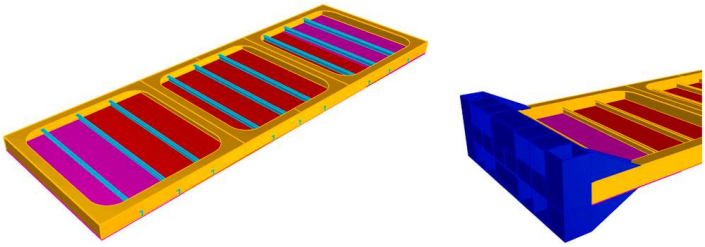

Fig. 2. 3D Geometry of the panel specimen and detail of the ends' stiffening structure.

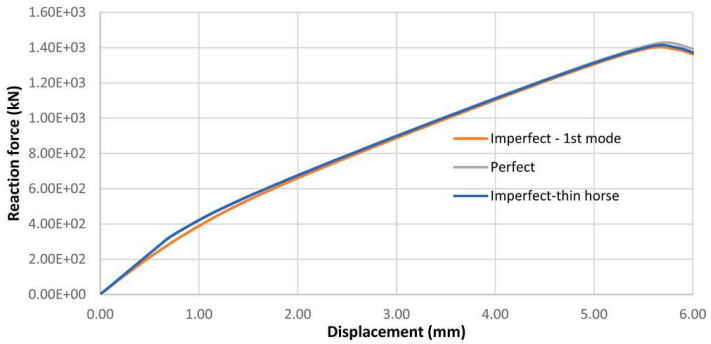

Fig. 3. Load end-shortening curves comparison.

Table 1
Ultimate strength capacity comparison.

MODEL	Ultimate Load [kN]	Percentage variation with respect to perfect model [%]
Perfect	1428.53	–
Imperfect - 1st mode	1402.46	−1.8 %
Imperfect-thin horse	1414.86	−1.0 %

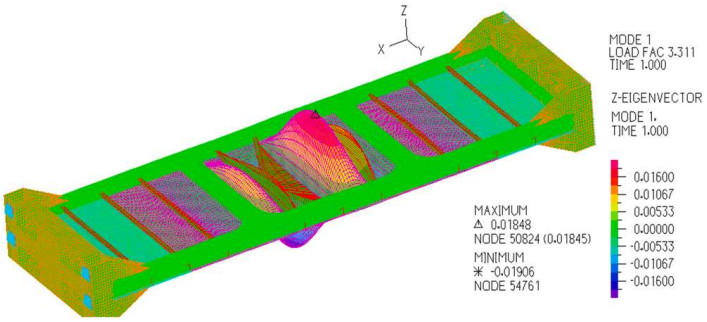

Fig. 4. 1st buckling mode imperfection shape.

while the residual stress evaluated analytically is equal to 15.02 MPa (see Section 6.2). Consequently, the residual stress alone in the direction of the load application should not lead to buckling of the panel during the manufacturing process. However, the combination of both residual stresses, perpendicular to each other, makes the 56.90 MPa of transverse residual stress exceeding the 38.96 MPa of capacity of the panel for combined stresses, evaluated according to analytical formulations, [16,17].

As it will be shown in Fig. 22a, the residual stresses induced by welding could have caused an initial deformation of the stiffened panel with a shape comparable the first Eigen-shape reported in Fig. 4, since they are larger than the elastic buckling strength of an elementary plate panel assumed simply-supported along all four edges by the stiffening members. Fig. 9 shows a graph which describes in detail the out of plane deformations of the plating along 3 bays and 7 longitudinal slices. Even if the initial imperfections are relatively high, they can be considered within the fabrication tolerances of ship structures [26]. In fact, the shipbuilding standard IACS Rec.47 [26] recommends panel fabrication with a limit of 8 mm in terms of plate imperfection between stiffening members and a standard of 4 mm. The panel manufactured by the shipyard according to usual practice shows geometric imperfections, as shown in Fig. 8 and 9, with deviations from the average plane of the plating reaching up to 6 mm in the most deformed areas, particularly in the two end intervals where a greater plating thickness was chosen to mitigate edge effects. Hence, the panel exceeds the IACS standard for

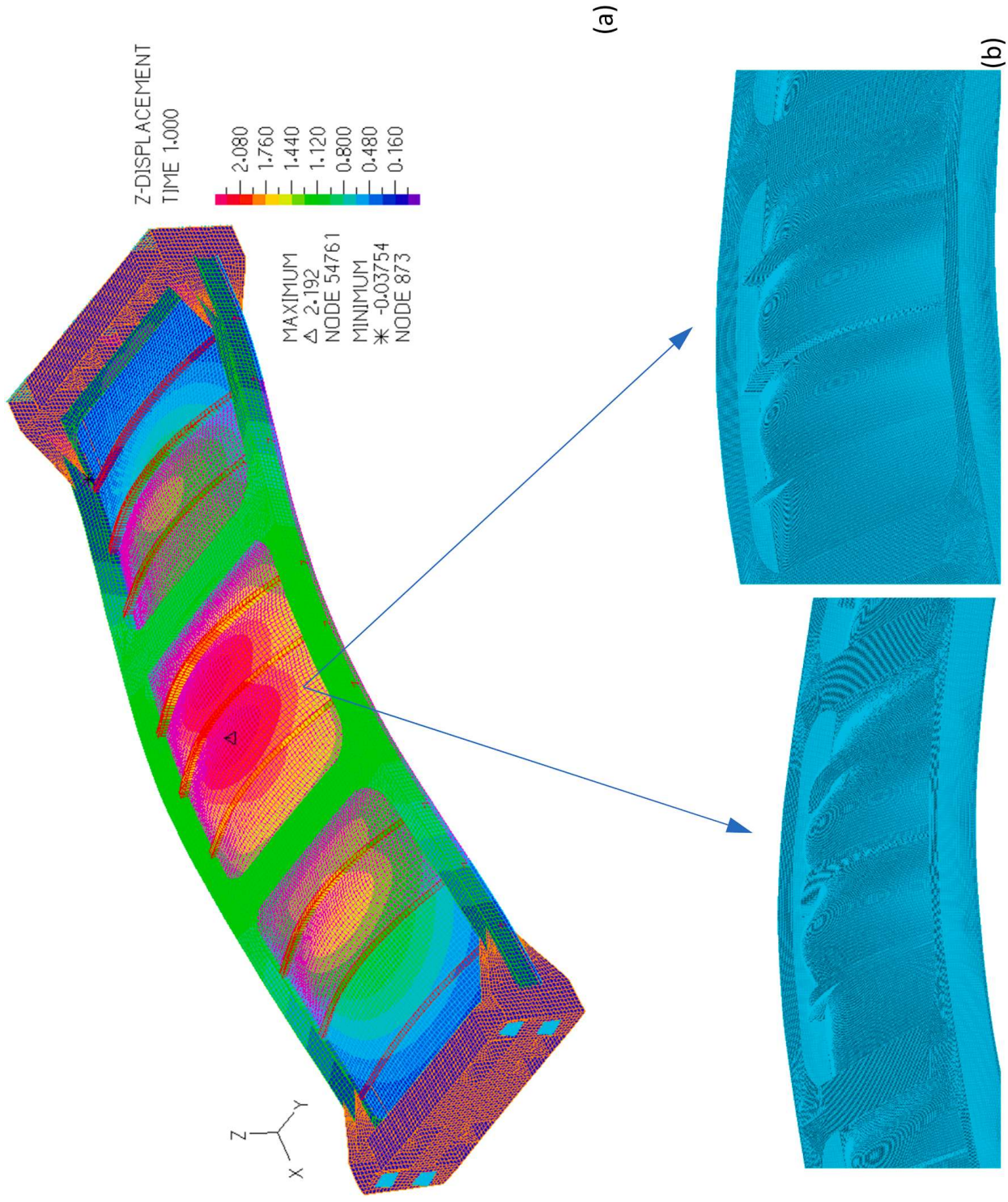

Fig. 5. (a) imperfection shape with global bending effect and (b) close up of the deformation in a bay showing the superimposed thin-horse imperfection shape.

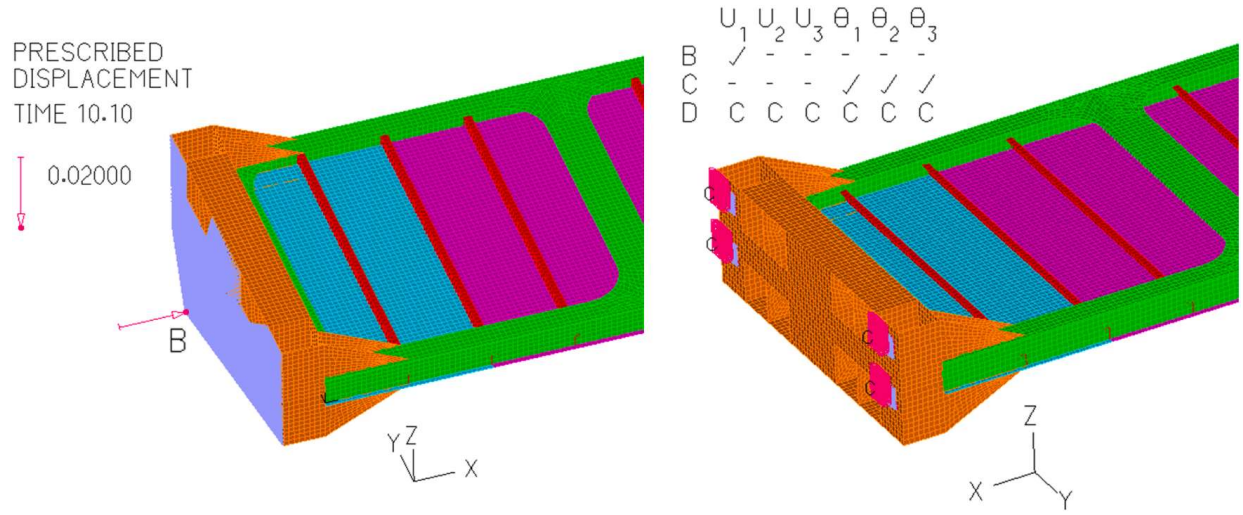

Fig. 6. Load application point (a, left) and fixity boundary conditions on the other edge (b, right).

fairness of plating between stiffeners but still complies with the imperfection limit.

3.2. Determination of actual thicknesses

Thickness measurements were performed with the OMNI-TM-8812 ultrasonic probe. It was found that the panel plating in the area of interest of the specimen, i.e. excluding the end parts that act as constraints condition, is thicker by 0.4 mm with respect to the 4.0 mm nominal value, with a non-negligible increase by 10 %, certainly contributing to modifying the structural response. The thicknesses of the webs and the flanges of the two side longitudinal beams were also measured, and a small deviation of only +0.1 mm was found.

These findings make it necessary to further update the preliminary analyses carried out so far, not only in order to predict the collapse conditions but also to evaluate with the best possible accuracy the areas in which to focus attention during the test to be carried out.

3.3. Actual material properties

After the first round of simulations that was due for the scantling of the panel to design the test and before its execution, in order to improve the reliability of the simulations, the actual material properties of the steel used for the specimen have been acquired via tensile tests of the lots of plates used for the construction. Such tests involved steel strakes having different thicknesses, ranging between 4 and 12 mm. Results obtained from the tests are shown in Table 2. Mean values and standard deviations are reported for the whole set of specimens but also calculated separately for the 4 mm and 10 mm sets, where the most of the specimens came from:

- Material Name: DH36
- Young Modulus: 205 [GPa]

In Table 3, the nominal material properties used in preliminary analyses for test design purposes (see Section 3) and the updated actual ones are shown. Note that material modulus is assumed to be the same as no data were available from tests.

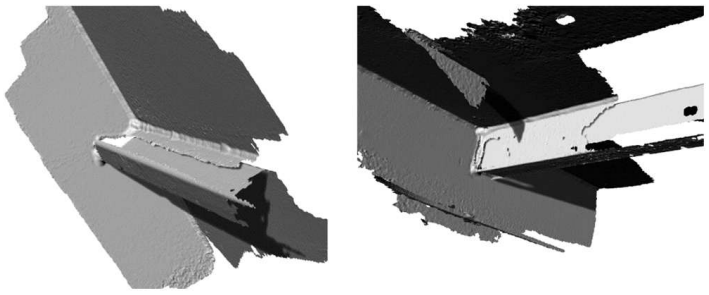

Fig. 7. Stiffeners scanning examples.

4. Updates of the numerical model based on the actual properties

The numerical model required modification to account for variations in material characteristics from nominal to actual values, as depicted in Table 3. Additionally, the geometry was updated to incorporate initial imperfections and the actual thicknesses of plating.

4.1. Material properties

Fig. 10 illustrates the modification of the end-shortening curve resulting from the enhancement of material properties. The impact of this alteration is readily apparent, as the actual material exhibits an increased ultimate capacity attributed to the higher tensile stress value.

4.2. Initial imperfections application

It is widely known that the imperfection pattern has also a great influence on the end-shortening curve, both in terms of ultimate strength and stiffness at the early stage. Fig. 11 reports the results for different modelling strategies of the initial geometry. In particular, the graph describes the results for the perfect model, the 1st buckling-mode shape imperfect model (as the one in Fig. 4) amplified for a maximum z-displacement of 5 mm (evaluated from the Fig. 8) and the model with the measured imperfection pattern. Unexpectedly, a greater drop in the stiffness is observed when modelling the actual imperfections, while the decrease in the ultimate strength with respect to the perfect model is quite similar to that observed for the 1st buckling mode shape.

5. Experimental test description

5.1. Test bench and data acquisition system

The experimental test has been conducted in the Marine Structures Testing Lab of the University of Genova, Italy. A test bench, 12 m long and 1.6 m wide, is available for static and dynamic testing of large- and full-scale specimens by applying forces up to 3000kN. The configuration of the testing condition is rather flexible and various equipment may be used to constrain the specimen. Hence, the collapse test was conceived and designed in detail according to the intended aims.

Fig. 12 shows the experimental setup ready for the test: the specimen panel has been placed on the test bench ready to receive the instrumentation for the collapse test. It is worth noting that the specimen during the test was not in contact with the test bench horizontal plane but only constrained on the vertical faces of the ends (own weight effect of the specimen was also considered in the numerical models but it was found negligible). The experiment is designed in order to have an infinitely rigid plate at the loaded end, which advances axially pushed by two actuators. The rigid constraint is specifically designed to introduce load without inducing end rotations: pure axial displacements are therefore rigidly transferred to the panel at its moving end.

The following sensors/transducers were installed for measurements during the test:

- 4 Allemano load cells model CC2S165100TC25, for measuring the load applied to the panel during the test, read as reaction force on the fixed edge of the specimen (Fig. 13a, b);
- 1 pressure sensor of the hydraulic circuit driving the actuators for the application of the axial load, measuring the load applied to the moving end of the specimen;
- 6 potentiometric displacement sensors (range 0 - 200 mm) suitable for detecting the axial displacements at different positions of the moving end of the specimen as well as that of the fixed end, if any (Fig. 14a);
- 40 strain gauge channels, including linear and rosette strain gauges (see exemplarily Fig. 14(b) showing a rosette 0°, ±45°, 90° on the top of shell plate) applied in significant points of the specimen, selected in accordance with the numerical analyses performed to design the test (Fig. 15). No strain gauges were installed in the external bays since they were designed and built to be totally rigid, being the core of this investigation the collapse of the stiffened panel, that happened in the central bay as expected, where all the 40 strain gauges were installed;
- Various centesimal mechanical comparators (accuracy 0.05 mm), useful for detecting possible flexibilities of the supporting structures and of the test bench, to validate the imposed constraint conditions.

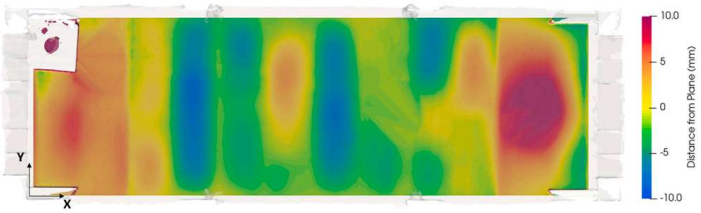

Fig. 8. Panel deviation from best-fit plane, top-down view.

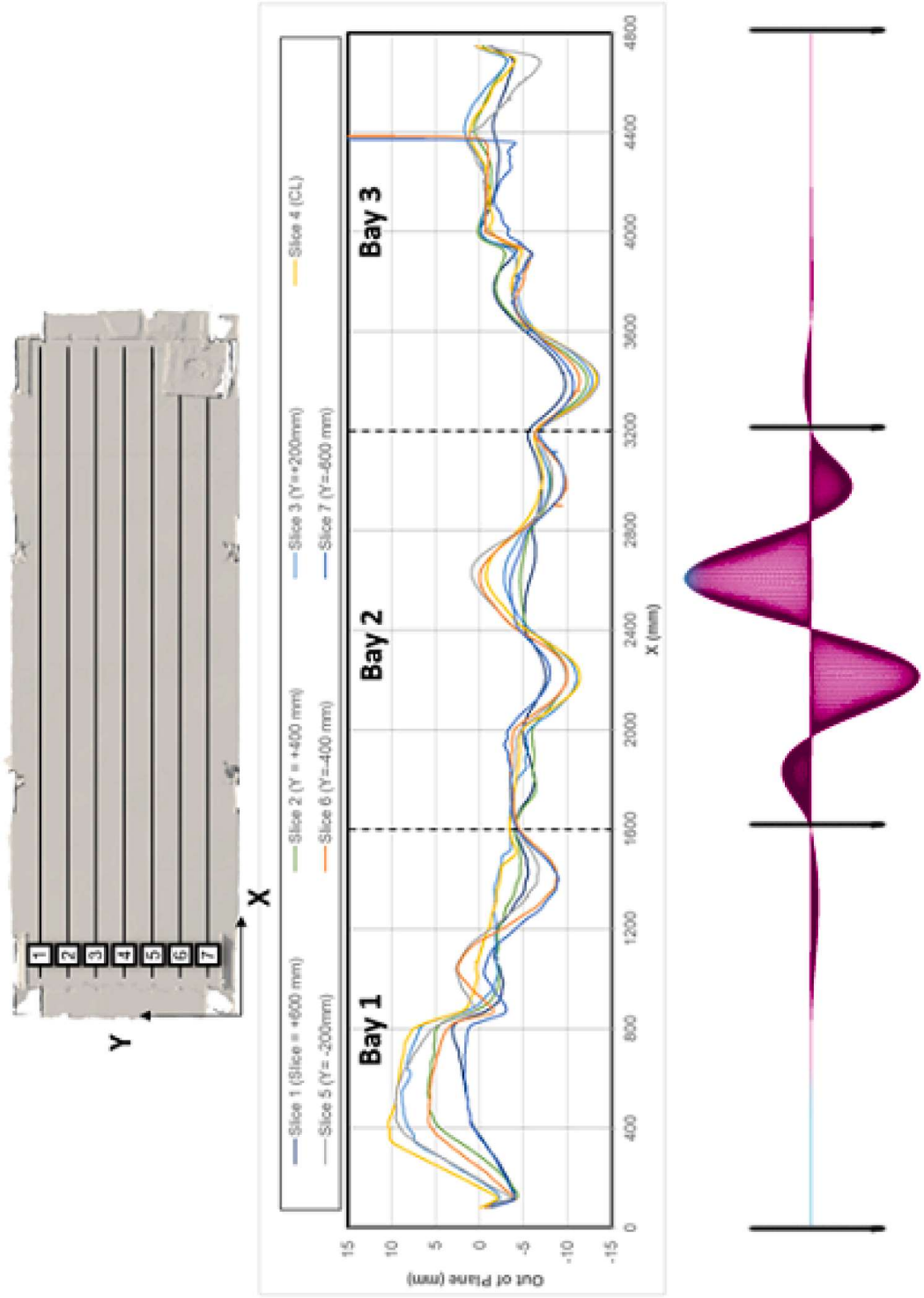

Fig. 9. Out of plane deformations along the plating and comparison with FEM 1st mode buckling shape of shell plating.

5.2. Collapse test

Before conducting the test, initial checks were performed to ensure proper alignments as well as instrumentation and equipment functionality. The test was carried out under force control by gradually increasing oil pressure on the actuators circuit using a pendulum machine with a slow load rate. This approach was taken to avoid sudden changes in axial displacement near the critical load and to enable the detection of the collapse curve (axial force-displacement) even after reaching the critical point. Prior to the test, a few load cycles were conducted within the elasticity limit of the stiffened panel specimen and well below the anticipated critical stress for local buckling. This aimed to recover any gap tolerances as far as possible and to verify the correct functioning of the equipment. During these load applications, measurements were taken using the acquisition system transducers and the acquired data were scrutinized to ensure the absence of any anomalies. It was particularly confirmed that the structure remained within its elastic regime.

Hence, sudden changes in displacement can only occur due to significant deformations in the specimen or imperfections in the boundary conditions at the fixed edge. This is because the specimen was firmly supported on the actuator side by a highly rigid moving plate along its entire lateral surface. The test concludes when the applied force exceeds a certain threshold, leading to a notable reduction in rigidity and causing excessive displacements that are beyond the capacity of the test equipment. Specifically, the test was halted upon observing a 30 % decrease in the applied force after reaching ultimate strength.

During the test, the following measurements were eventually taken:

- Axial displacement of the loaded edge of the specimen in three points, to check applied load direction besides panel shortening;
- Axial displacement of the fixed edge of the specimen in three points, to evaluate possible deformation of the supporting structure, if any;
- Data acquired by four load cells on the fixed edge, specifically designed also to provide vertical support to the panel; this also allowed to overcome possible uncertainties led by friction of specimen's constraining structures;
- Load applied by the two actuators, namely by acquiring the oil pressure on the loaded edge, to be compared by the axial load measured by the load cells to evaluate friction and also to provide backup data on the applied loading;
- 40 measurements of different strain components, acquired by 16 strain linear and rosette gages.
- Two HD Videos of the shell plating acquired by different angles with markers on plating, suitable for 3D reconstruction.

6. Load redistribution and modelling of welding induced residual stresses

Upon initial examination of the experimental results regarding structural response, it is evident that the side longitudinal girders, accounting for approximately 30% of the total transverse section area of the panel, bear 75% of the applied compressive load, while the plate experiences minimal load. This observation is based on the strain gauge results (specifically, e.g. on strains measured by gauges A, E, and M), which indicate significantly greater strains in the longitudinal beam flange compared to the panel plating, as shown exemplarily in Fig. 16.

Table 2
Tensile test data, actual mechanical properties of the specimens

Specimen #	Thickness [mm]	Yield Strength [MPa]	Engineering Tensile Strength [MPa]	Elongation at break [%]
1	**4**	417	505	38.2
2	**4**	394	495	40.2
3	**4**	416	499	34.1
4	**4**	382	502	34.7
5	**4**	385	493	33.5
6	**4**	412	495	36.9
	Average	401	498	36.27
	St. Dev.	14.54	4.26	2.39
7	**5**	398	494	39.4
8	**6**	387	497	38.3
9	**8**	399	529	31.8
10	**10**	395	546	28.2
11	**10**	406	532	34.1
12	**10**	397	529	35.5
13	**10**	396	526	30.1
14	**10**	389	533	28.7
	Average	397	533	31.32
	St. Dev.	5.46	6.85	2.94
15	**12**	425	554	32.8
16	**12**	392	550	29.8
Overall	Average	399	517	34.14
	St. Dev.	**12.48**	**22.08**	**3.79**